New electro-optic logic gate design and computer graphics spectrum

Zhang Yang[1], Liu Haiyan[2]

(1. Beijing Information Technology College, Beijing 100055, China;
2. Department of Water Resources and Hydropower Engineering, Tsinghua University, Beijing 100010, China)

Abstract: An optical logic gate is the core of optical information processing in all future optical network elements, allowing for high-speed optical packet switching, all-optical address identification, data coding, parity, and signal regeneration. A micro-ring resonator was adopted to design a new electro-optical logic gate using three asymmetric micro-rings. The analysis of coupled transfer matrix equations showed that the change in the load voltage signal resulted in a change in the refractive index. Micro-rings using the logic-switching characteristic of light intensity can achieve an optical logic gate. The computer simulation verified that the working wavelength was 1 600 nm. The high-level load voltage 50.7 V was defined as logic 1, whereas the low-level load voltage was defined as logic 0. A voltage of 0 V was obtained by six light intensity change logic operations. The response time of the entire system is 1.8 ps theoretically, and the computation speed can reach approximately 200 Gbit/s. The bistable logic analysis revealed that the micro-ring is equal to the corresponding control micro-ring at maximum resonant wavelength. No deformation occurred in the resonant wavelength and the sum of the offset. Therefore, modulation can be achieved through micro-ring resonant wavelength control.

Key words: optical network; optical logic gates; micro ring resonator; coupling area
CLC number: O23 **Document code:** A **DOI:** 10.3788/IRLA201746.0122003

新型电光逻辑门的设计及计算机图形光谱

张 洋[1],刘海燕[2]

(1. 北京信息职业技术学院,北京 100055; 2. 清华大学 水利水电工程系,北京 100010)

摘 要: 光逻辑门是未来全光网络中光信息处理的核心元件,它可以实现高速光包交换,全光地址识别,数据编码,奇偶校验,信号再生等功能。采用微环谐振器设计了一种新型的电光逻辑门,结构通过三个非对称微环组成, 分析耦合区的传输矩阵方程得出加载电压信号的变化能够实现微环折射率的变化,利用光强的逻辑开关特性可以实现光门逻辑。计算机仿真验证了工作波长 1 600 nm 时,实现的高电平 50.7 V 定义为逻辑 1,低电平 0 V 定义为逻辑 0,通过光强变化得出了 6 位逻辑运算;整个系统的响应时间理论上得到了 1.8 ps,运算速率可达近 200 Gbit/s。逻辑的双稳态分析中得出:微环发生最大谐振值时对应的控制波长等于微环未发生形变前的谐振波长和偏移量之和; 调制可以通过微环谐振波长实现控制。这一研究对于未来全光通信的实现具有一定的意义。

收稿日期:2016-05-05; **修订日期**:2016-06-03
基金项目:国家自然科学基金(10674041)
作者简介:张洋(1979),女,讲师,硕士,主要从事图形图像方面的研究。Email:ludunlu902@163.com

关键词：全光网络； 光逻辑门； 微环谐振器； 耦合区

0 Introduction

In recent years, new optical fiber communication devices as well as production and plane waveguide technologies have experienced continuous enhancement because of their decreasing cost[1-3]. Micro-ring resonators have undergone rapid development theoretically and experimentally and serve as building blocks in the implementation of integrated photonic devices and as important basis of optical waveguides[4-5]. The resonance effect of circular waveguides has special characteristics, such as wavelength selection and high quality factor. At present, micro-ring resonators have been extensively applied to the production of laser frequency modulators, optical waveguide multiplexers, biological chemical sensors, modulators, and optical switches[6]. Marcatili proposed the concept of resonant micro-ring in 1969[7]. Given its small size, compact structure, low dissipation, and high wavelength selectivity, optical micro-ring resonators have various practical applications, including optical signal processing, filtering, wavelength division multiplexing modulation, switching, and routing. In practical applications, the ideal output spectrum of a micro-ring resonator output is a "box" spectrum[8]. However, the currently reported structures of ring resonators cannot completely satisfy this requirement. Accordingly, many scholars have used multiple micro-rings in series or parallel to solve the disadvantages of monocycles. Scholars have also adopted parameters based on the optimal arrangement of rings or changed the micro-rings to optimize the output waveform[6]. In 2004, Chen et al., from the University of Maryland, analyzed the characteristics of a micro-ring system by employing a matrix method, which uses the recursive relationships between different light propagation paths, and deduced all the paths of the transfer function. Based on the above background, in this paper, we design a new type of electro-optic logic gate. The results show that the method of the multi-function logic gate can be designed for future large-scale optical logic unit assembly and design provides convenient.

1 Structure design and theoretical analysis

1.1 Micro-ring transmission characteristics

The micro-rings of the input and output ports are high, and the ring of light is the traveling wave. The working diagram is shown in Fig.1. In the ring and straight waveguide coupling area, the mode-coupling matrix can be used to describe the assumptions for the micro-ring coupling coefficient k, and the transmission coefficient for the micro-ring t, under the coupling condition $k^2+t^2=1$.

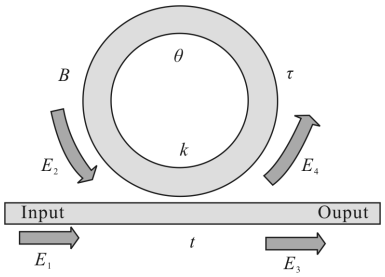

Fig.1 Model for the micro-ring

The light from one end of the straight waveguide input or energy E_1 is part of the input energy coupled to the ring; this is a part of the output from the other end of the optical waveguide. The transmission of energy E_2 from the ring part continues to spread in the ring; another part is coupled to the waveguides and lost in the output end. The analysis indicates that the relationship between E_1 and E_2 can be described using the following transfer matrix:

$$\begin{pmatrix} E_1 \\ E_2 \end{pmatrix} = \begin{pmatrix} t & k \\ -k^* & t^* \end{pmatrix} \begin{pmatrix} E_1 \\ E_2 \end{pmatrix} \tag{1}$$

We set E_1 to 1 to simplify the model. Light propagation as a result of ring loss satisfies the following relation:

$$E_2=\tau\cdot e^{j\theta}E_4 \tag{2}$$

If the micro-ring radius is denoted by R, the inside process for transmission coefficient denoted by τ, the effective refractive index of the waveguide denoted by n_{eff}, the longitudinal propagation constant light waves denoted by β, the light wave angular frequency denoted by w, the speed of light in a vacuum denoted by c, the wavelength denoted by λ, the micro-ring cavity length denoted by L, and transmission time for the micro-ring denoted by t, then the following equations can be derived:

$$\beta=k\cdot n_{\text{eff}}=\frac{2\pi\cdot n_{\text{eff}}}{\lambda}$$

$$\theta=k\cdot n_{\text{eff}}\cdot 2\pi r=\frac{2\pi n_{\text{eff}}\cdot 2\pi r}{\lambda}=\frac{4\pi^2 r n_{\text{eff}}}{\lambda} \tag{3}$$

From the Equation (3), the expression for the power of the ring can be derived as follows:

$$P_3=|E_3|^2=\frac{\tau^2+t^2-2\pi\cos\theta}{1+\tau^2t^2-2\pi\cos\theta}$$

$$P_4=|E_4|^2=\frac{\tau^2(1-t^2)}{1+\tau^2t^2-2\pi\cos\theta} \tag{4}$$

When $\theta=2m\pi$, the ring is resonant. Formula (4) shows that a given integer will correspond to a specific wavelength. Thus, when ring resonance occurs, a series of corresponding wavelengths exists.

1.2 Structure design

Figure 2 shows the electro-optical logical structure designed in this study to achieve a variety of logical relationships. The structure is composed of three loops. The straight waveguide and door waveguide connect every two micro-rings. We use coupled mode theory and transfer matrix method to establish a mathematical model that can be employed to determine the switch characteristics and obtain the output spectrum. If the coupling coefficient k and the transmission coefficient t of the three coupled micro-rings are the same, then the six transfer equations for the coupled zones can be expressed as follows:

$$\begin{bmatrix}A_2\\B_2\end{bmatrix}=\begin{bmatrix}\frac{t}{jk} & -\frac{1}{jk}\\ \frac{1}{jk} & -\frac{t}{jk}\end{bmatrix}\begin{bmatrix}A_1\\B_1\end{bmatrix},\ \begin{bmatrix}C_1\\D_1\end{bmatrix}=\begin{bmatrix}\frac{t}{jk} & -\frac{1}{jk}\\ \frac{1}{jk} & -\frac{t}{jk}\end{bmatrix}\begin{bmatrix}C_2\\D_2\end{bmatrix},$$

$$\begin{bmatrix}E_2\\F_2\end{bmatrix}=\begin{bmatrix}\frac{t}{jk} & -\frac{1}{jk}\\ \frac{1}{jk} & -\frac{t}{jk}\end{bmatrix}\begin{bmatrix}E_1\\F_1\end{bmatrix},\ \begin{bmatrix}G_1\\H_1\end{bmatrix}=\begin{bmatrix}\frac{t}{jk} & -\frac{1}{jk}\\ \frac{1}{jk} & -\frac{t}{jk}\end{bmatrix}\begin{bmatrix}G_2\\H_2\end{bmatrix},$$

$$\begin{bmatrix}I_2\\J_2\end{bmatrix}=\begin{bmatrix}\frac{t}{jk} & -\frac{1}{jk}\\ \frac{1}{jk} & -\frac{t}{jk}\end{bmatrix}\begin{bmatrix}I_1\\J_1\end{bmatrix},\ \begin{bmatrix}K_1\\K_1\end{bmatrix}=\begin{bmatrix}\frac{t}{jk} & -\frac{1}{jk}\\ \frac{1}{jk} & -\frac{t}{jk}\end{bmatrix}\begin{bmatrix}L_2\\L_2\end{bmatrix} \tag{5}$$

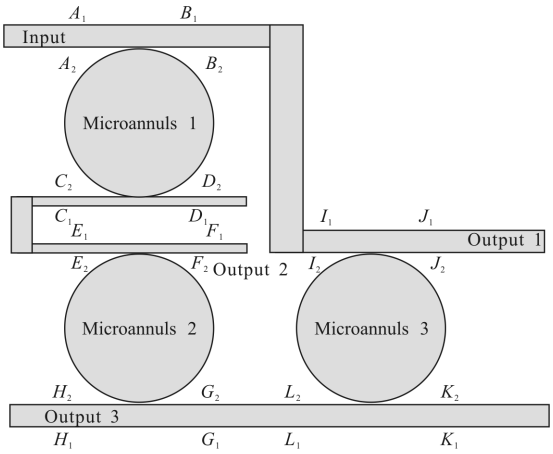

Fig.2 Logical system structure

Given a ring for the loss α_R, the transfer matrices for the three micro-rings can be expressed as follows:

$$\begin{bmatrix}C_2\\D_2\end{bmatrix}=\begin{bmatrix}0 & \exp(-j\varphi)\\ \exp(j\varphi) & 0\end{bmatrix}\begin{bmatrix}A_2\\B_2\end{bmatrix},$$

$$\begin{bmatrix}G_2\\H_2\end{bmatrix}=\begin{bmatrix}0 & \exp(-j\varphi)\\ \exp(j\varphi) & 0\end{bmatrix}\begin{bmatrix}E_2\\F_2\end{bmatrix},$$

$$\begin{bmatrix}K_2\\L_2\end{bmatrix}=\begin{bmatrix}0 & \exp(-j\varphi)\\ \exp(j\varphi) & 0\end{bmatrix}\begin{bmatrix}I_2\\J_2\end{bmatrix} \tag{6}$$

The phase factor is expressed as $\phi=\pi R(\beta-j\alpha_R)$, where R is the micro-ring radius and β is the transmission coefficient. If the micro-ring waveguide bending loss α_1 is set to 1 and 2; the micro-ring waveguide loss α_2 is set to 2 and 3; and the straight waveguide loss is disregarded, then the waveguide glazing field intensity transfer relationships for the micro-rings are expressed as follows: $I_1=B_1$, $E_1=\exp(-j\pi R\ (\beta-j\alpha_1))D_1$, and $G_1=\exp\ (-j\pi R\ (\beta-j\alpha_2))L_1$. According to these relations, the three outlets for the output light field of the normalized output optical field intensity can be derived. In this study, an appropriate micro-ring material selection is recommended for the electro-optical polymer with linear electro-optical effect. The core layer of electro-optical polymer materials for the refractive index change is expressed as follows:

$$\Delta n_{10}=\frac{1}{2}n_{10}^{3}r_{33}E_1=\frac{n_{10}^{3}n_{20}^{3}r_{33}U}{2(2n_{10}^{2}d_2+n_{20}^{2}d_1)} \tag{7}$$

where U denotes the electrode at the end of the load voltage. According to Equations (5)–(7), the load voltage signal changes can cause a change in the refractive index. The resonant wavelengths of the three micro-rings of the light switch can be determined. Thus, the logic circuits can be used to derive the logic operations.

2 Structure analysis

2.1 Logical calculation

On the basis of the relations and mathematical models derived in the previous section, a computer graphics software-aided simulation calculation of the logic circuit is conducted. Table 1 lists the different load voltages of the micro-rings for a given output spectrum.

Tab.1 Load voltage

	Micro-ring 1	Micro-ring 2	Micro-ring 3
Load voltage/V	0	0	0
	0	0	50.7
	0	50.7	0
	0	50.7	50.7
	50.7	0	0
	50.7	0	50.7
	50.7	50.7	0
	50.7	50.7	50.7

As a result, the logic value is defined as 010. The output spectrum wavelength glazing strong logical value of the corresponding work is shown in Tab.2.

Tab.2 Logic circuit input and output table value of true

Micro-ring logic value output logic	Output logic
000	001
001	010
010	001
011	100
100	100
101	100
110	010
111	010

2.2 Micro-ring characteristic simulation

We need to obtain the refractive index distribution of the waveguide cross section to verify the correctness of the waveguide parameters. The refractive index distribution is shown in Fig.3. Simulation is shown in Fig.4.

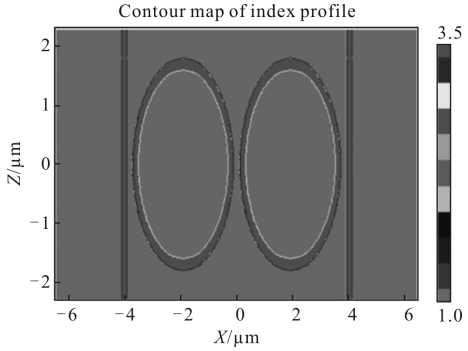

Fig.3 Waveguide refractive index distribution of the cross section

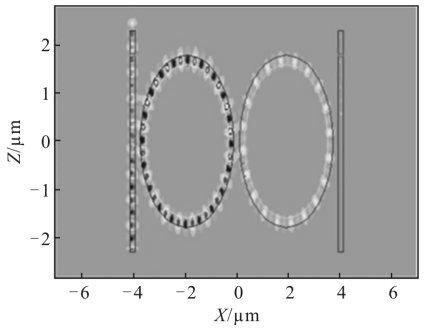

Fig.4 Simulation diagram

The simulation verified that the logic variety of a door can be implemented in the logic circuits. Given that the electro-optical polymer micro-ring switch response time is short, i.e., 0.5 ps, the response time of the entire system should be approximately 1.8 ps. If the length of the input and output waveguides is 1 000 μm, including the length of the waveguide, then the operation of the device delay time is 5.5 ps and the operation rate can reach approximately 200 Gbit/s.

2.3 Logic realization of bistability

When different methods are employed to control the wave modulation input into the straight waveguide and micro-rings, different phenomena will occur. In this section, these phenomena are discussed and explained. When the control wavelength gradually increases from 1600 nm, the entire process is as follows:

the wave energy coupled to the ring is controlled, the light force is produced, the light force of the ring is bent, ring bending leads to an effective refractive index change in the ring, the ring of the resonant frequency changes, and optical coupling energy results from the change in the resonant frequency of the light reaction force. This process is a mutual coupling process. To solve this problem, we assume that, at the given control wavelength of the wave, the loop energy does not change. However, when the wavelength increases, the next time point of the resonant frequency of the ring more than a moment after the change shall prevail. Under the condition of a given control wavelength, given that the micro-ring bending degree is small, the experiment and simulation show that the degree of variation in dozens of nano-ring and micro-ring resonant frequencies is not evident. However, the relationship between the coupled powers also indicates that the small change in the value of the micro-ring energy is less; thus, we do not consider the condition of an energy change in a ring of a given wavelength. After adjusting the parameters and the control wavelength gradually increases from the 1 600 nm wavelength modulation, the final stable wavelength is 1 604 nm. This experimental result is largely in line with the results of Fig.5.

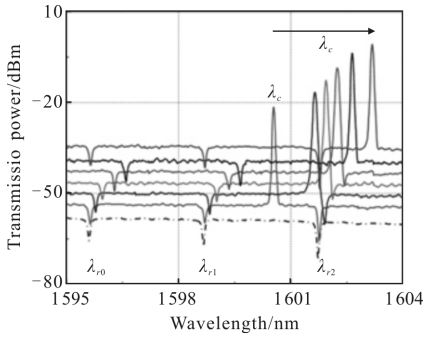

Fig.5 Control wavelength increase data graph

It can been seen from Fig.5 that when the control wavelength gradually increases from left to right, the resonant wavelengths of the three corresponding micro-rings will increase. When the control wavelength is longer than 1 604 m, the resonant wavelength of the micro-ring does not change, indicating that micro-ring resonance occurs at this time. When the control wavelength increases from 1 604 nm, wavelength increase in the principal process is reduced. The difference is that, when the wavelength reduces the micro-ring curve, which leads to an increase in the resonant frequency, the wavelength difference will soon decay to zero. Therefore, when the relative control wavelength increases, its ultimate resonant wavelength will decrease and the resonant frequency value of the resonator will become smaller. The theoretical and experimental data shown in Fig.6 are consistent.

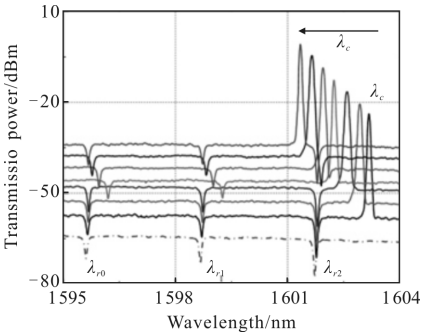

Fig.6 Control wavelength decrease data graph

It can be seen from Fig.6 that when the control wavelength decreases from right to left, the resonant wavelengths of the three corresponding micro-rings will increase. When the control wavelength is shorter than 1 602 nm, the micro-ring resonant wavelength is restored to its original position. The experimental data show that the extreme is reached at 1 602.3 nm. The modulation chart of the two modulation processes is finally obtained and shown in Fig.7.

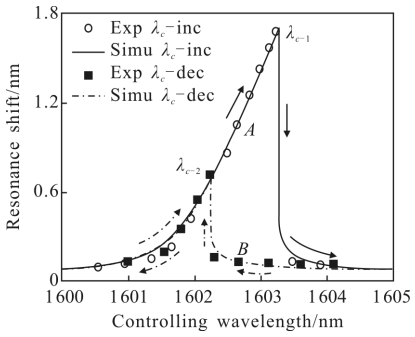

Fig.7 Hysteretic diagram

The solid line in the graph represents the modulation wavelength that increased from 1 600 nm to 1 600 nm, which shows the change in the deviation of the resonant micro-ring. The blue line in the graph represents the modulation wavelength that increased from 1 605 nm to 1 605 nm, which shows the change in the deviation of the micro-ring. In the integrated calculation and theoretical analysis, we observed the following pattern: a micro-ring is evident when the maximum resonant wavelength is equal to the corresponding control micro-ring before deformation occurred in the resonant wavelength and the sum of the offset. This phenomenon is evident in the calculation process. When the control wavelength and the resonant wavelength are equal, the maximum deformation in the micro-ring occurs; subsequently, the micro-ring will rapidly return to its initial position. The solid line corresponds to the maximum control wavelength, whereas the blue line corresponds to the minimum control wavelength. This outcome is determined by the control of the wavelength modulation process. When the modulation wavelength gradually increases, the resonant wavelength of the micro-ring extends, and its initial value is higher than those of the resonant wavelength of the modulation wavelength. The increase in wavelength modulation amplitude is higher than that of the resonant wavelength. Thus, after several iterations, an equilibrium value is eventually reached. When the modulation wavelength decreases, the resonant wavelength of the micro-ring still increases; as a result, an equilibrium value is reached. The modulation offset represented by the solid line is greater than that represented by the dotted line.

3 Conclusion

Based on the micro ring resonator, we design a variety of logic gate function which can be realized the electro-optical logical circuit. The structure can replace the SOI material which make switch using electro-optic polymer faster response time, less loss, and saving material and to decrease the size of the device. In this paper, through the simulation calculation show that the logical circuit which can realize the function of the six kinds of logic gate. Only by varying inlet and outlet can get different logical functions, the design of logic gate can future large-scale optical logic unit assembly and design provides convenient.

References:

[1] Zhu W, Tian Y, Zhang L, et al. Directed xor/xnor logic gates using U –to –U waveguides and two microring resonators[J]. ***IEEE Photonics Technology Letters***, 2013, 25 (1): 18–21.

[2] Lentine A L, Mccormick F B, Novotny R A, et al. A 2 kbit array of symmetric self-electrooptic effect devices [J]. ***IEEE Photonics Technology Letters***, 1990, 2: 51 – 53.

[3] Kumar S, Singh G, Bisht A, et al. Proposed new approach to the design of universal logic gates using the electro-optic effect in Mach-Zehnder interferometers. [J]. ***Applied Optics***, 2015, 54(28): 8479–8484.

[4] Xing Jiejiang, Li Zhi yong, Yu Yude, et al. Low cross-talk 2×2 silicon electro-optic switch matrix with a double-gate configuration[J]. ***Optics Letters***, 2013, 38(22): 4774.

[5] Kumar A, Raghuwanshi S K. Realization of optical digital magnitude comparator using electro-optic effect based cascaded mach-zehnder interferometer structure [J]. ***Journal of Nanoelectronics & Optoelectronics***, 2015, 10(6):1–10.

[6] Zhu M, Zhou Z, Gao D. Silicon electro-optic modulator with high-permittivity gate dielectric layer [J]. ***Chinese Optics Letters***, 2009, 7(10):924–925.

[7] Kumar A, Kumar S, Raghuwanshi S K. Implementation of full-adder and full-subtractor based on electro-optic effect in Mach-Zehnder interferometers [J]. ***Optics Communications***, 2014, 324: 93–107.

[8] Zhu Jun, Qin Liuli, Song Shuxiang, et al. Design of a surface plasmon resonance sensor based on grating connection [J]. ***Photonic Sensors***, 2015, 5(2): 159–165.